Sixth International Conference on Durability of Concrete Structures **Paper Number PSE09**
18 - 20 July 2018
University of Leeds, Leeds, West Yorkshire, LS2 9JT, United Kingdom

Effect of Corrosion and Corrosion rate on the Mechanical Performance of Carbon and Stainless Steel Reinforcing Bars

H.L. Wang, X.Y. Sun and H.T. Kong
Department of Civil Engineering, Zhejiang University, Hangzhou, China

ABSTRACT

Steel corrosion is a predominant factor leading to age-related structural degradation. To understand the different effects of pitting corrosion on the mechanical performances of deformed carbon and stainless steel reinforcing bars, an artificially accelerated method was conducted to corrode the steel bars. Using a 3D laser scanner, the three-dimensional models of corroded steel bars were reconstructed. The corrosion characterization was identified based on these 3D profiles. The results indicate that the number and the depth of corrosion pits of both types of steel increase with the increase of corrosion rate, however the pitting corrosion of stainless steel is much more obvious than the carbon steel. Axial tensile tests of corroded carbon and stainless steel bars were carried out. The tensile test results show that both the yield and ultimate loads linearly decreased with an increase of corrosion loss while the ductility decreased correspondingly. With the increase of corrosion loss, brittle fracture gradually occurred in the corroded carbon steel bars at the location of critical cross-sectional area. However, the degradation ratio of elongation of stainless steel is less than that of the carbon steel.

Keywords: Corrosion characteristic, mechanical property, area loss, ductility, 3D profile.

1.0 INTRODUCTION

Corrosion of steel bars is the main cause of durability degradation of reinforced concrete (RC) structures. Many investigations indicated that corrosion will lead to the loss of the rebar area, change the deboning performance between rebar and concrete, and deteriorate the mechanical properties of the structure (Zhao *et al.*, 2014; Tang *et al.*, 2014). To resolve the corrosion problem, the use of stainless steel reinforcements seem to be the most reliable solutions to guarantee the durability of RC structure existing in the aggressive environments (Knudsen *et al.*, 1998; Castro-Borges *et al.*, 2002). Using stainless steels can essentially improve the corrosion resistance of embedded bars, because the alloy elements of chromium, nickel and molybdenum can form a more stable oxide layer protecting the metallic matrix beneath the film away from chloride corrosion. Many studies have been explored to discuss the corrosion resistance of stainless steel (Fajardo *et al.*, 2011; Freire *et al.*, 2011; Bertolini *et al.*, 2014), but few of them considered the corrosion effect on the mechanical performance of stainless steel reinforcing bar.

Up to now, numerous literatures reported the corrosion behavior of carbon steel, however owing to the limitation on corrosion detection, most of the investigations are based on the hypothesis of uniform corrosion. Actually, pitting corrosion is the most common corrosion form in the RC structures, especially in the stainless steel reinforced concrete structures. Compared with general corrosion, the presence of pitting corrosion can lead to significant decreases in structural reliability for RC members (Stewart, 2004; Stewart and Al-Harthy, 2008), and even worse, the pits can undergo brittle failure instead of plastic failure that will likely elicit serious consequences (Darmawan and Stewart, 2004). Therefore, accurate measurements on the corrosion pit are crucial for steel assessments and structural analyses. However, the conventional methods such as mass weighting and caliper cannot precisely assess the pitting corrosion of the corroded rebar.

Since pitting corrosion is the commonest corrosion morphology of carbon and stainless steel reinforcing bars, accurate measurement of the corrosion characteristic of the steel was conducted using a 3D laser scanner in this study. Then, the corrosion differences of carbon and stainless steel reinforcing bars are compared. To explored the pitting corrosion on the mechanical performances of deformed carbon and stainless steel reinforcing bars, axial tensile tests of corroded steel bars were carried out.

2.0 EXPERIMENTAL PROGRAMME

2.1 Specimen Preparation

The specimens were prepared using a hot-rolled ribbed (HRB) steel bar and a duplex 2204 stainless steel reinforcing bar. The nominal diameters of the bars were 16 mm. The specimens were prepared to

be approximately 500 mm long. To avoid the corrosion and the fracture of the two gripped ends in the tensile test, the two ends of the specimens were coated with epoxy.

Direct electric current (DC) was impressed on the steel bar to accelerate the corrosion of the steel reinforcing bar with the use of a DC power supply. The reinforcements were connected to the positive end, and a stainless metal mesh was connected to the negative end of the power supply. The NaCl solution with 5% concentration by mass was used to provide a corrosive environment. The applied current density i was 400 μA/cm^2 in each case. After the expected corrosion times, the corrosion products of the steel bars were removed using a steel brush. Then the specimens were cleaned with dilute hydrochloric acid, neutralised with $Ca(OH)_2$ solution, washed with clean water, and kept in a closed dry container until the 3D profile measurement and the tensile test.

2.2 Corrosion Measurements Based on 3D Scanning

The surface morphology of all corroded bars was measured using a 3D laser scanner to establish the 3D profile and determine the remaining cross-section. The scanning speed is 37 mm/s, and the positioning accuracy is 0.02 mm. The sampling distance of the vertical region is 400 mm. As shown in Fig. 1, the three-dimensional coordinates of the points on the surface of the rebar was acquired by the laser scanning instrument, and processed by the scanning system's software to form a point cloud file. Then the software Geomagic was then used to build the solid model of the corroded bars on the basis of the point cloud file.

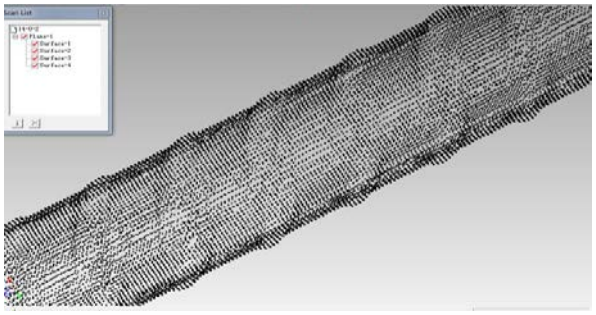

Fig.1. Point cloud of reinforcing bar from scanning

After the establishment, a software Pro Engineer was then used to analyse the sectional area of the corroded bars for every 1 mm along their length, thereby allowing estimation of the cross-sectional area loss.

2.3 Tensile Test

The axial tensile test was performed at all levels of selected corrosion at ambient temperatures using a servo-hydraulic testing system, as shown in Fig.2. The load was measured by the load cell of the test machine, while the displacement was acquired by a linear variable differential transformer. All readings were recorded using an automatic data acquisition system, and were used to plot the load-displacement curve. The yield strength and the ultimate tensile strength of corroded bars were determined based on the corresponding test curve. To evaluate the corrosion effect on the ductility properties of the reinforcing steel bar, the percentage elongation after fracture was calculated as the ratio of the extension between two marks placed near the fracture area with respect to the initial length.

Fig.2. Axial tensile test

3.0 RESULTS AND DISCUSSION

3.1 Evaluation of Corrosion Parameters

The representative 3D images of corroded carbon and stainless steel bars are displayed in Fig.3. The distributions of cross-sectional areas along the length of the reinforcing bars corresponding to Fig.3 are plotted in Fig.4. As shown in Fig.4, the corrosion distribution along the length becomes more irregular, and the number and depth of corrosion pits increases when the corrosion rate increases. The corrosion pit is narrow and deep in the stainless steel bars for the reason that pitting corrosion is the dominate corrosion morphology of stainless steel. To characterise the non-uniform distribution of corrosion, the degree of maximum corrosion η_{crt} was obtained from image analyses, the average mass loss η_m was gotten by weighing, while the uniformity coefficient was defined as R. They can be calculated from following formula.

$$\eta_{\mathrm{m}} = \frac{M_0 - M}{\rho_l L} \tag{1}$$

$$\eta_{crt} = \frac{A_0 - A_{\min}}{A_0} \tag{2}$$

$$R = \frac{A_{ave}}{A_{\min}} \tag{3}$$

Where M_0 and M are the masses of the bars before and after corrosion, ρ_l is the line density of the bars, L is the length of the corrosion part, A_0 is the average sectional area of the control group, A_{min} is the minimum sectional area of the corroded bars, and A_{ave} is the average sectional area of the corroded bars.

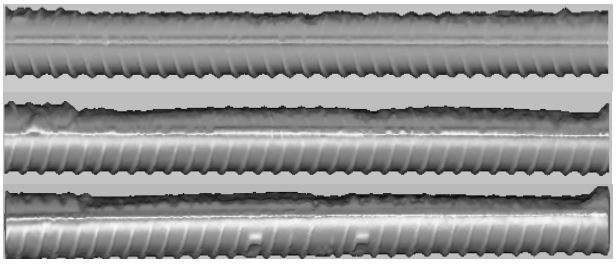

(a) Carbon steel bars

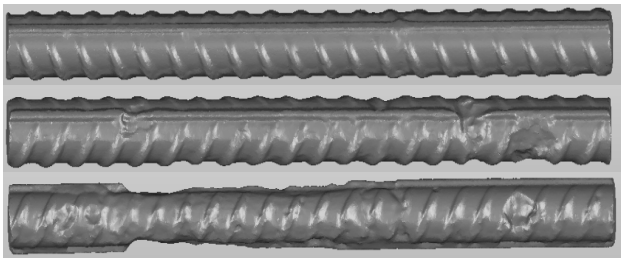

(b) Stainless steel bars

Fig. 3. Representative 3D images of corroded reinforcing bars

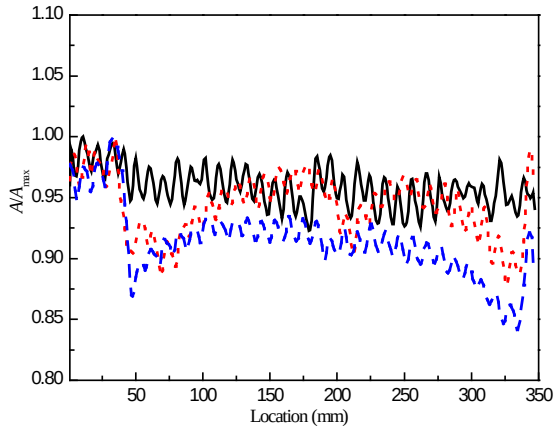

(a) Carbon steel bars

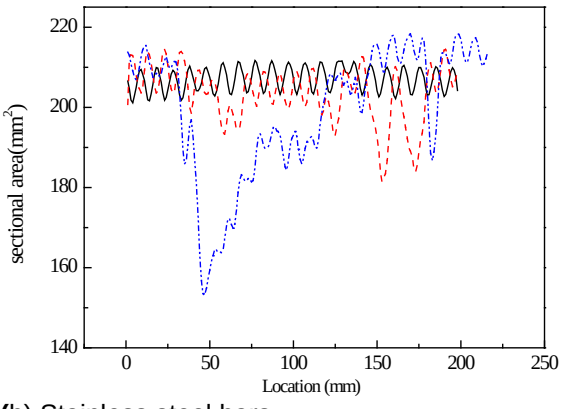

(b) Stainless steel bars

Fig. 4. Corrosion distribution along the bars' length

The variation trends of the non-uniform coefficient R are illustrated in Fig.5. As the corrosion level increases, the non-uniform coefficient R increases, and attains discrete values at high corrosion levels for carbon steel. The higher value of R means the higher degree of corrosion irregularity or more corrosion pit in the steel. As displayed in Fig.5, the value R for stainless steel is obviously higher than that of the carbon steel. It is evidenced again that the pitting corrosion is the prominent corrosion morphology in the stainless steel. Therefore, the local corrosion parameters instead of the average mass loss should be used to identify the corrosion effect on the mechanical properties of steel bars.

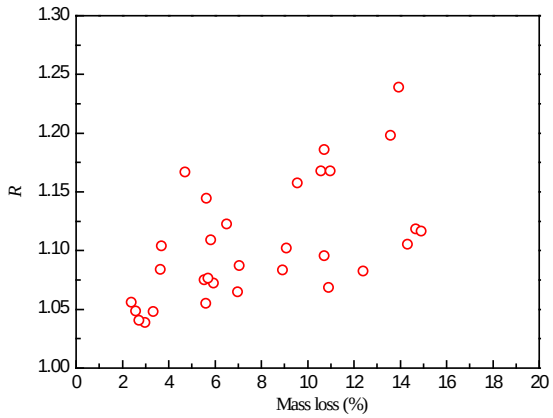

(a) Carbon steel bars

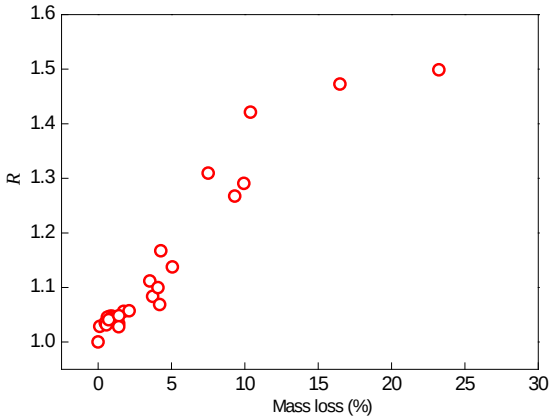

(b) Stainless steel bars

Fig.5. Variation of heterogeneous coefficient R

3.2 Corrosion Effect on Strengths

As it is known, there is serious stress concentration around the corrosion pit, which influences the mechanical properties of corroded steel. To clarify the impact of pitting corrosion, the maximum cross-sectional corrosion rate is adopted in this study to clarify its effect on the performance degradation of steel bar based on the 3D profile.

Based on the yield and ultimate strengths of the carbon and stainless steel bars, the ratios of the strengths of corroded steel to uncorroded steel, known as the relative yields and ultimate strengths,

can be calculated. The degradation of the relative yields and ultimate strengths are plotted in Figs.6 and 7. It can be seen that both the yield and ultimate loads decreased linearly with increases of corrosion loss. The strength's degradation ratio of stainless steel is more pronounced than that of the carbon steel due to its deeper corrosion pit.

As shown in Figs.6 and 7, both the yield and ultimate strength of corroded bars can be expressed as follows:

$$f_{yc} = \left(A_y - \alpha_{yc}\eta_{crt}\right) f_{y0} \tag{10}$$

$$f_{uc} = \left(A_u - \alpha_{uc}\eta_{crt}\right) f_{u0} \tag{11}$$

Where α_{yc} and α_{uc} are regression constants obtained from the experimental strength results and from η_{crt}. As stated above, for 3D scanning profiles, the cross-section can be captured by inserting a plane perpendicular to the centerline of the steel bar, and the degree of maximum corrosion can be evaluated precisely according to Eq. (2). From this point-of-view, the prediction model in this study is more reliable.

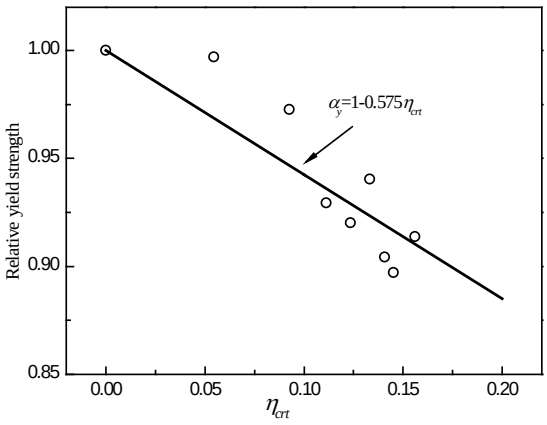

(a) Relative yield strength

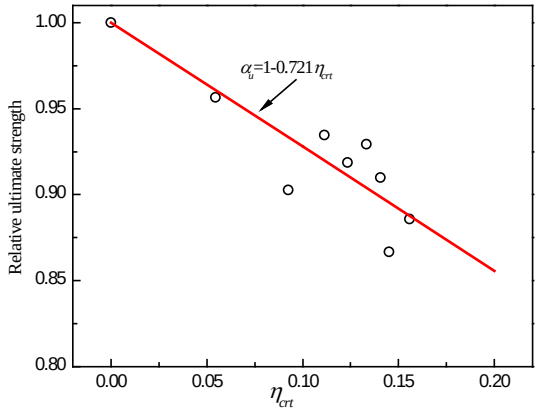

(b) Relative ultimate strength

Fig.6. Strength degradation of corroded carbon steel

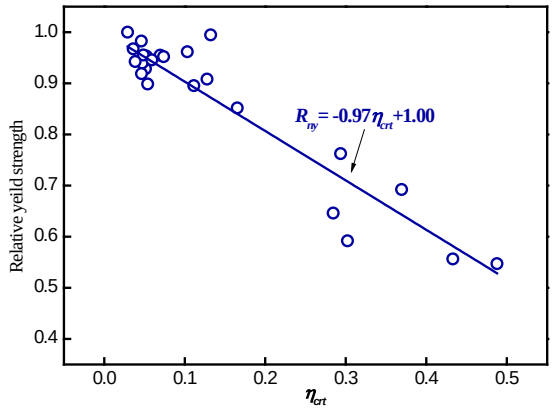

(a) Relative yield strength

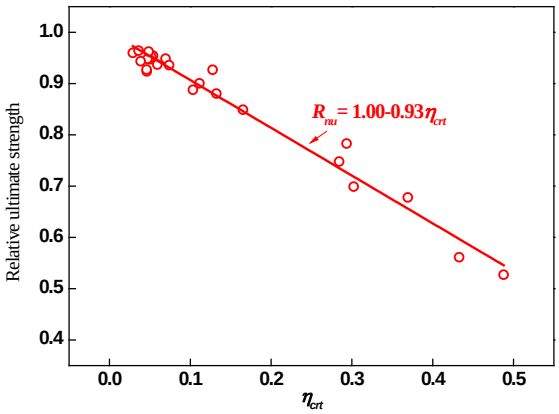

(b) Relative ultimate strength

Fig.7. Strength degradation of corroded stainless steel

3.3 Corrosion Effect on Ductility

The measured elongation is normally used to directly represent the ductility of reinforcing steel bars. The final gauge lengths of the rebars after fracture were recorded in the test. The percentage elongations are illustrated in Fig.8. It can be seen that the elongation of the corroded bar decreases with increasing degrees of corrosion. As illustrated in Fig.8a, a linear function can be adopted to describe approximately the effect of the degree of maximum corrosion on the ductility of the corroded carbon steel bars. Compared the degradation ratios of ductility and strengths, it can be seen that the pit corrosion has a more profound effect on the ductility of reinforcing steel bars rather than on their strengths.

As displayed in Fig.8b, an exponential function can be used to identify the corrosion effect on the ductility of the stainless steel bars. Compared the curves of Figs.8a and 8b, it is clear that the pit corrosion has a significant effect on the ductility of carbon steel bars because the addition of alloy elements in the stainless steel enhance its ductility greatly.

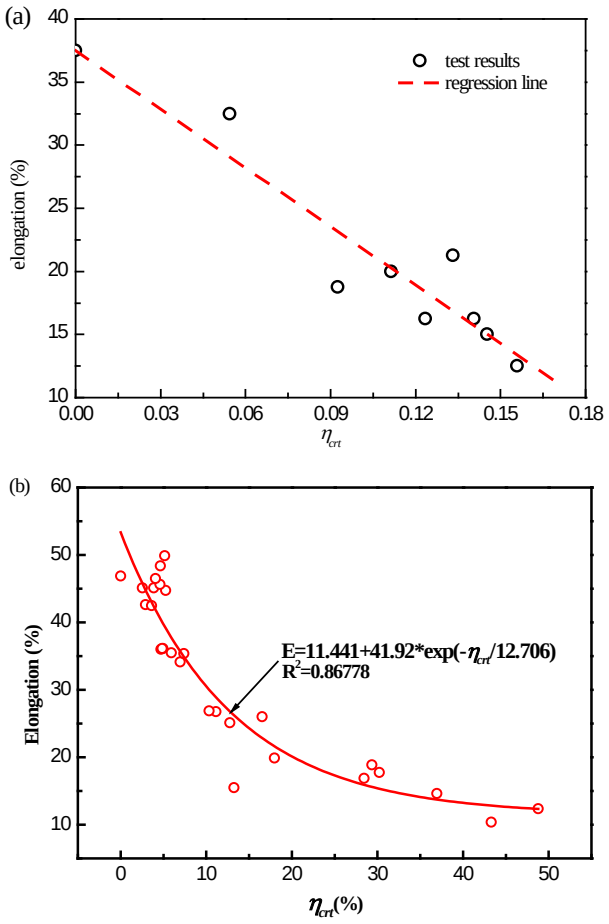

Fig.8. Degradation of the elongation: (a) carbon steel, and (b) stainless steel

It was also found from the experiment that brittle fracture gradually occurred in the corroded carbon steel bars with the increasing corrosion. It is also verified that the corroded steel bars suffer a significant ductility loss.

4.0 CONCLUSIONS

Pitting corrosion is the dominant corrosion morphology of stainless steel. The corrosion pit of stainless steel is more narrow and deeper than that of the carbon steel.

Both the yield and ultimate strengths of carbon and stainless steel linearly decreased with the increase of cross section due to corrosion. However, the strength degradation ratio of stainless steel is more pronounced than that of the carbon steel due to its deeper corrosion pit.

Pitting corrosion had an obvious effect on the ductility of reinforcing steel bars, and the ductility loss was much more significant than strength degradation.

Compared with the carbon steel bar, the stainless steel bar has a better ductility. Even under severe corrosion conditions, the stainless steel can still maintain a certain elongation, which can prevent the brittle failure of RC structures.

Acknowledgement

The authors are grateful for the financial support received from the National Natural Science Foundation of China (51579220), the National High Technology Research and Development Program (863Program) of China (2015AA03A502), and the Natural Science Foundation of Zhejiang Province (LY16E080004).

References

Bertolini, L., Bolzoni, F., Pastore, T. *et al.*, 2014. Behaviour of stainless steel in simulated concrete pore solution. Brit. Corros. J., 31(3):218-222(5).

Castro-Borges, P., Rincón, O. T. D., Moreno, E. I., *et al.*, 2002. Performance of a 60-year old concrete pier with stainless steel reinforcement. Mater Perform, 41(10):50–55.

Darmawan, M.S., Stewart, M.G., 2004. Spatial variability of pitting corrosion and its effect on the strength and reliability of prestressed concrete bridge beams. Cds.cern.ch..

Fajardo, S., Bastidas, D. M., Criado, M., *et al.*, 2011. Corrosion behaviour of a new low-nickel stainless steel in saturated calcium hydroxide solution. Constr. Build. Mater., 25(11):4190–4196.

Freire, L., Carmezim, M. J., Ferreira, M. G. S., *et al.*, 2011. The electrochemical behaviour of stainless steel AISI 304 in alkaline solutions with different pH in the presence of chlorides. Electrochim Acta, 56:5280–5289.

Knudsen, A., Jensen, F. M., Klinghoffer, O., *et al.*, 1998. Cost-effective enhancement of durability of concrete structures by intelligent use of stainless steel reinforcement. Conference on corrosion and rehabilitation of reinforced concrete structures, Florida, USA.

Stewart, M., 2004. Spatial variability of pitting corrosion and its influence on structural fragility and reliability of RC beams in flexure. Struct. Safe. 26:453-470.

Stewart, M., Al-Harthy, A., 2008. Pitting corrosion and structural reliability of corroding RC structures: Experimental data and probabilistic analysis. Reliab. Eng. Syst. Safe., 93:373-382.

Tang F, Lin Z, *et al.*, 2014. Three-dimensional corrosion pit measurement and statistical mechanical degradation analysis of deformed steel bars subjected to accelerated corrosion. Constr. Build. Mater., 70:104-117.

Zhao, Y., Dong, J., *et al.*, 2014. Steel corrosion and corrosion-induced cracking in recycled aggregate concrete. Corros. Sci. 85:241-250.